frontiers in Materials

ORIGINAL RESEARCH
published: 14 December 2018
doi: 10.3389/fmats.2018.00074

Commercial Fiber Products Derived Free-Standing Porous Carbonized-Membranes for Highly Efficient Solar Steam Generation

Xiaofeng Lin, Meijia Yang, Wei Hong, Dingshan Yu* and Xudong Chen**

Key Laboratory for Polymeric Composite and Functional Materials of Ministry of Education of China, Guangdong Engineering Technology Research Center for High-performance Organic and Polymer Photoelectric Functional Films, School of Chemistry, Sun Yat-sen University, Guangzhou, China

Herein, the free-standing porous carbonized-membranes (CMs) derived from a series of commercial fiber products including airlaid papers, cellulose papers and cleanroom wipers by one-step carbonization at 160°C have for the first time explored as independent solar absorbers to realize highly efficient solar steam generation. These newly-developed CMs not only exhibit the strong absorption (low reflectance) and rapid transport of vapor/liquid, but also possess the restricted thermal diffusion. All these merits render CMs with excellent evaporation performance for solar steam generation. Particularly, the CMs derived from carbonized cellulose papers (CCPs) exhibits the best performance, which affords the water evaporation rate of 0.959 $kg{\cdot}m^{-2}{\cdot}h^{-1}$ and the energy conversion efficiency of 65.8% under 1 $kW{\cdot}m^{-2}$ solar illumination, due to the higher light absorption (92.20%) and lower thermal conductivity (0.031 W·m-1·K-1) competing favorable with those of the Au nanoparticles-loaded airlaid papers (Au-APs, 0.856 $kg{\cdot}m^{-2}{\cdot}h^{-1}$, 58.7%). Due to the low-cost, recyclability and highly efficient evaporation performance, the CMs, especially the CCPs, show great potential as solar absorbers for large-scale application of solar steam generation.

Keywords: solar absorber, solar steam generation, porous membrane, fiber products, photothermal conversion

OPEN ACCESS

Edited by:
Dong Wook Chang,
Pukyong National University,
South Korea

Reviewed by:
Dong Ryeol Whang,
Johannes Kepler University of Linz,
Austria
In-Yup Jeon,
Wonkwang University, South Korea

****Correspondence:***
Dingshan Yu
yudings@mail.sysu.edu.cn
Wei Hong
hongwei9@mail.sysu.edu.cn
Xudong Chen
cescxd@mail.sysu.edu.cn

Specialty section:
This article was submitted to Energy Materials, a section of the journal Frontiers in Materials

Received: *04 October 2018*
Accepted: *27 November 2018*
Published: *14 December 2018*

Citation:
Lin X, Yang M, Hong W, Yu D and Chen X (2018) Commercial Fiber Products Derived Free-Standing Porous Carbonized-Membranes for Highly Efficient Solar Steam Generation. Front. Mater. 5:74. doi: 10.3389/fmats.2018.00074

INTRODUCTION

The solar steam generation as one of the most promising technology for the water scarcity (Shannon et al., 2008; Elimelech and Phillip, 2011; Ni et al., 2016), which focuses on the effective conversion from solar energy to thermal energy, has attracted a lot of research attention (Elimelech and Phillip, 2011; Zhou et al., 2016c). Such hopeful and efficient technology of light-to-heat conversion can be widely used in the field of purification of drinking water, domestic water heating (Ghasemi et al., 2014; Ni et al., 2016), solar desalination (Zhu et al., 2016; Liu et al., 2017), absorption chillers (Schiermeier, 2008; Philibert, 2011; Lewis, 2016), and sewage treatment (Liu et al., 2015b; Lou et al., 2016), etc. Nevertheless, the traditional techniques of the solar steam generation generally rely on complicated and costly optical concentrators to enhance the water evaporation, leading to a large number of energy loss and the maintenance expense of the facilities in the long term (Karagiannis and Soldatos, 2008; Lenert and Wang, 2012; El-Agouz et al., 2014; Liu et al., 2015c). Therefore, it is necessary for solar steam generation to exploit more cost-effective and efficient evaporators.

Generally, the highly efficient solar steam generation strongly depends on the efficient light-absorbers in the evaporators. In the previous studies, the plasmonic (Wang et al., 2014; Bae et al., 2015; Liu et al., 2015c; Zhou et al., 2016b, 2017), and carbon-based materials (Ito et al., 2015; Zhou et al., 2016a; Hu et al., 2017), have been extensively studied among the reported absorbers due to their remarkable solar-thermal conversion efficiency. Nevertheless, in order to lower the cost and increase the evaporation efficiency, most previous reports usually added low-cost/insulated supports [e.g., airlaid paper Liu et al., 2015c, 2017; Lou et al., 2016; Wang et al., 2017a,b] with effective light-absorbing materials [e.g., carbon black (Liu et al., 2015a, 2017) and gold nanoparticles (Liu et al., 2015c; Wang et al., 2017b)] to construct the multilayer-composite absorbers. However, the composite structures often suffer from the costly preparation (complex process) and interfacial barriers to heat/mass transfer, which would be adverse to the large-area industrial manufacture (Lin et al., 2018). Therefore, ideal solar absorbers should not only afford the high light-to-heat conversion efficiency for the efficient solar steam generation, but also render cost-effective and facile preparation for the large scale industrial manufacture.

Due to the low-cost and high-abundance, the commercial fiber products, such as the airlaid papers (APs), cellulose papers (CPs) and cleanroom wipers (CWs), have been used in cleaning of the optical/medical devices, batteries separators, and solar steam generation (Nyholm et al., 2011; Xu et al., 2015; Wang et al., 2017a,b). They could not only be a great support layer for absorbing materials, but also have great potential to be an independent solar absorber without any additive of absorbing layer, owing to the advantages of lightweight, mechanical stability, and low thermal conductivity (Liu et al., 2017).

In this work, we demonstrate that the free-standing porous carbonized-membranes (CMs) derived from the commercial fiber products (e.g., APs, CPs, CWs) via the one-step carbonization at 160°C, for the first time, can be directly used as independent solar absorbers to realize highly efficient solar steam generation. Our proposed CMs could show multiple advantages to promote the evaporation efficiency including strong absorption (low reflectance) due to the carbonization, rapid transport of vapor/liquid because of the porous structure, and restricted thermal diffusion ascribed to low thermal conductivity. As expected, the carbonized cellulose papers (CCPs) with higher light absorption (92.20%) and lower thermal conductivity (0.031 $W \cdot m^{-1} \cdot K^{-1}$) as our optimal CMs yields the highest water evaporation rates (0.959 $kg \cdot m^{-2} \cdot h^{-1}$) and energy conversion efficiency (65.8%) under 1 $kW \cdot m^{-2}$ solar illumination, competing favorable with those of the Au nanoparticles-loaded airlaid papers (Au-APs, 0.856 $kg \cdot m^{-2} \cdot h^{-1}$, 58.7%).

EXPERIMENTAL

Materials

The commercial cellulose papers were purchased from Kimberly-Clark Corporation (USA, 34155 KIMWIPES) with a size of 11 cm × 21 cm. The commercial airlaid papers were purchased from CLEANROOM (China, WIP-0609) with a size of 22.86 cm × 22.86 cm. The commercial cleanroom wipers (polyester fiber) were purchased from CLEANROOM (China, WIP-2009) with a size of 22.86 cm × 22.86 cm.

Preparation of Au Nanoparticles-loaded Airlaid Papers (Au-APs)

Synthesis of the Au Nanoparticles

Au-APs were firstly produced based on the literature reported method (Liu et al., 2015c). Typically, 50 mL of 1 mM $HAuCl_4$ aqueous solution (prepared by Chloroauric acid tetrahytrate, Sinopharm Chemical Reagent Co., Ltd., 99.99%) was added into a round-bottom flask (100 mL) with a condenser and boiled with vigorous stirring. Subsequently, 5 mL of 38.8 mM sodium citrate solution (Guangzhou Chemical Reagent Factory) was added into the $HAuCl_4$ aqueous solution. We note that the color of mixture solution turned from pale yellow to kermesinus. Afterwards, the mixture solution was boiled for 15 min and kept stirring (stop heating) for 1 h until the solution cooled down. Finally, the aqueous solution of colloidal Au nanoparticles was obtained.

Loading of the Au Nanoparticles on Airlaid Papers

The preparation of Au-APs were described as follows: a piece of clipped AP was placed at bottom of the 100-mL beaker. Afterwards, the beaker was filled with 30 mL of colloidal Au nanoparticles aqueous solution. Simultaneously, the beaker together with a petri dish filling with 10 mL of formic acid (Guangzhou Chemical Reagent Factory) was placed inside a sealed desiccator at room temperature. After 48 h, the Au nanoparticles film could be formed at the air-water interface. Followed by extracting the solution between the bottomed AP and the Au nanoparticles film, the film would be coated onto the AP. Finally, the Au-APs were achieved by drying at 50°C in the oven.

Preparation of CMs

In a typical experiment, a piece of fabric (including APs, CPs, CWs) was dipped into the H_2SO_4:water:ethanol mixture solution (1:25:60, volume ratio) and was heated in an oven for 4 h under the normal atmosphere at 160°C. Finally, after washing by the deionized water, various CMs were achieved via drying.

Characterization of Materials

The UV-Vis diffuse reflectance spectra and transmittance spectra of the CMs were measured using a UV/VIS/NIR spectrophotometer (UV3600, Shimadzu) combined with an integrating sphere (ISR-3100). The absorptance was calculated by A = 1-R-T, where R and T were the reflectance and transmittance, respectively. The surface compositions of the CMs were measured with a photo-electron spectroscopy (XPS, ESCALAB 250, Thermofisher Scientific) equipped with a monochromatic X-ray source (Al Kα, 1486.6 eV). The contents of the C, H, S, O of the CMs were tested by the Elemental Analyzer (EA, Vario EL, Elementar). The field emission scanning electron microscopy

(FE-SEM, Hitachi S-4800) was used to obtain the SEM images. The thermal conductivity of the CMs were measured by a thermal conductivity measuring instrument (TPS 550 S, Hot disk). The concentrations of Fe^{3+}, Al^{3+}, Cr^{3+}, Cu^{2+}, Mn^{2+}, and Ni^{2+} of the CMs were measured using plasma atomic emission spectrometry (ICP-AES, IRIS(HR), TJA).

Test System for Solar Steam Generation

The light source of the test system was generated by a 300 W xenon lamp (simulated solar irradiation, Microsolar 300, Perfectlight), which was calibrated by a photoradiometer (PL-MW2000, Perfectlight). The change of the mass was accurately recorded by an electronic balance (AR224CN, OHAUS) coupled with a computer for the calculation of the water evaporation rate. Simultaneously, an infrared radiation (IR) camera (T420, FLIR) monitored the real-time temperature for the final calculation of energy conversion efficiency.

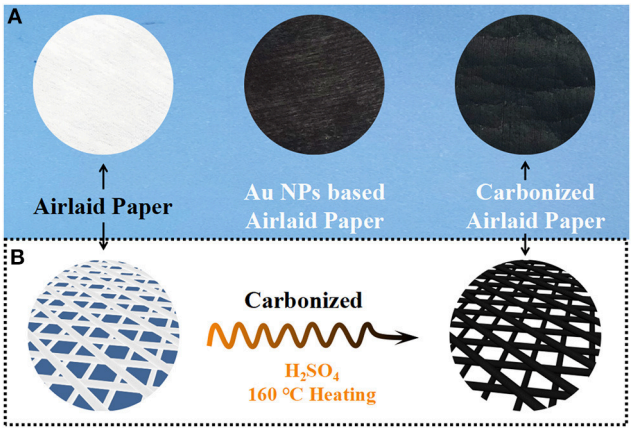

FIGURE 1 | (A) The photographs of APs, Au-APs and CAPs. **(B)** The fabrication process of the carbonized airlaid paper.

RESULTS AND DISCUSSION

In the previous reports, the APs was often used as a substrate to support the plasmonic absorbers or the carbon-based absorbers for notable water evaporation efficiency, respectively. The increased surface roughness of the APs substrate could cause the multiple scattering of incident solar light, leading to the high absorption of the sunlight. Simultaneously, the porous structure of the APs could potentially utilize the capillarity to facilitate the water forward the hot zone, resulting in the rapid supplement for the loss of the surface water evaporation. Moreover, airlaid paper also could be as a good thermal insulator to prevent the thermal loss because of the low thermal conductivity (Liu et al., 2015c, 2017). However, the composite structures could suffer from the complicated preparation and interfacial barriers to heat/mass transfer (Lin et al., 2018). Therefore, the commercial fiber products such as APs might be directly applied as a light-to-heat conversion absorber for solar steam generation.

For this purpose, the carbonized airlaid paper (CAPs), which were based on the precursor of commercial APs (composed of 55% cellulose and 45% polyester), have been chosen. In order to inherit the porous structure and lightweight (ca. 80 $g{\cdot}m^{-2}$, see in **Supplementary Table S1**), the CAPs were directly obtained from APs through a simple carbonized process using H_2SO_4:water:ethanol mixture solution (**Figure 1**) in an oven under the normal atmosphere. The CAPs could sufficiently retain the porous structures as evidenced by the scanning electron microscopy (SEM) images in **Supplementary Figure S1**. The samples were of low densities and could safely float on the surface of the water. Such open-pore structure would provide transportation channels for the rapid transport of vapor and liquid (Hu et al., 2017; Lin et al., 2018). Moreover, due to the specific microstructures of APs, the local convection would be suppressed during the water evaporation (Liu et al., 2015c; Lin et al., 2018).

As shown in the schematic diagram in **Figure 2** and the photograph in **Supplementary Figure S2**, the test system of the solar steam generation ability for the CMs consists of a simulated solar irradiation, a weighing module and a temperature monitoring system. The CMs with a diameter of ca. 4 cm was floated on the surface of the water in a weighing bottle, which was located on the electronic balance under the light source. When subjected to the illumination, the mass change of water during the solar steam generation was detected by the weighing module, which was equipped with the electronic balance and the computer. Simultaneously, the real-time temperature on the surface of the CMs was measured by an infrared radiation (IR) camera (ambient temperature:25°C and humidity: 50%).

The typical curves of the mass change vs. time under 1 sun illumination ($C_{opt} = 1$, solar illumination with a power density of 1 $kW{\cdot}m^{-2}$) for different samples are exhibited in **Figure 3A**, while the water evaporation rates ($\dot{m}$) are calculated from the slope of the curves (**Supplementary Table S1**). Under the solar illumination with a power density of 1 $kW{\cdot}m^{-2}$, the average water evaporation rates of CAPs were measured to be 0.924 $kg{\cdot}m^{-2}{\cdot}h^{-1}$, ca. 2.1 times those of pure water (0.431 $kg{\cdot}m^{-2}{\cdot}h^{-1}$) and APs (0.440 $kg{\cdot}m^{-2}{\cdot}h^{-1}$). Moreover, another reference sample of the Au-APs (shown in **Figure 1A**) was fabricated to obtain an evaporation rate of 0.856 $kg{\cdot}m^{-2}{\cdot}h^{-1}$, which was lower than that of CAPs (0.924 $kg{\cdot}m^{-2}{\cdot}h^{-1}$). Compared with previous reports (Liu et al., 2015c, 2017; Lou et al., 2016; Wang et al., 2017a,b). the optimal evaporation rate of CAPs (0.924 $kg{\cdot}m^{-2}{\cdot}h^{-1}$) representsone of the best AP-based solar absorbers' results for solar steam generation under similar temperature and humidity ($C_{opt} = 1$, 25°C, 50%).

However, it is well-known that the characteristics of the cellulose, such as the thermal conductivity and absorbency, are obviously different from that of the polyester (Idicula et al., 2006), while the composition of the APs is 55% cellulose and 45% polyester. Therefore, it indicates that optimizing the content of the commercial fiber products' cellulose and polyester could effectively improve their thermal conductivity and absorbency, in order to help reduce heat loss and increase the utilization of solar energy that the potentially improve the solar steam generation ability of the CMs (Hu et al., 2017). The commercial CPs (100%

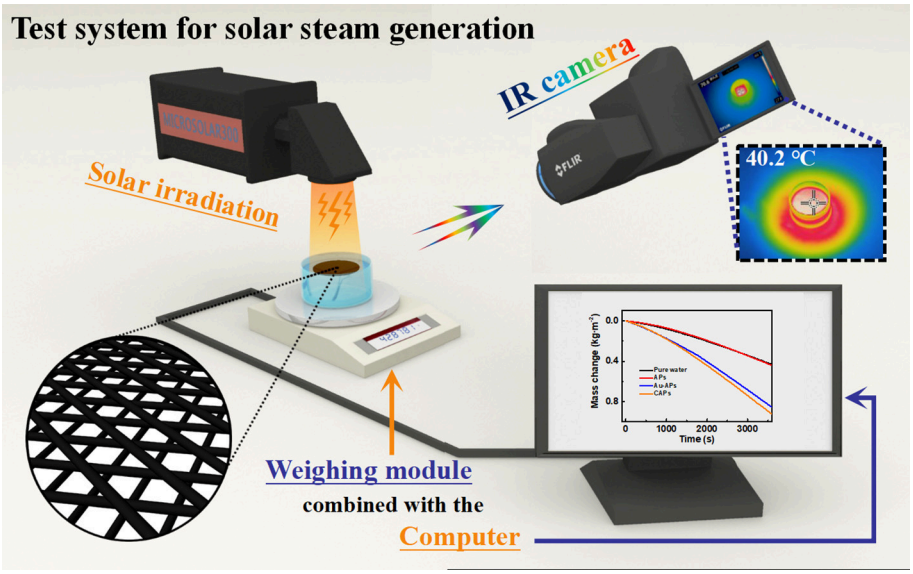

FIGURE 2 | The schematic diagram of the test system for solar steam generation ability. Bottom left corner: the schematic of the free-floating CMs on the water contained in a weighing bottle; Top right corner: the IR image of the CMs under illumination.

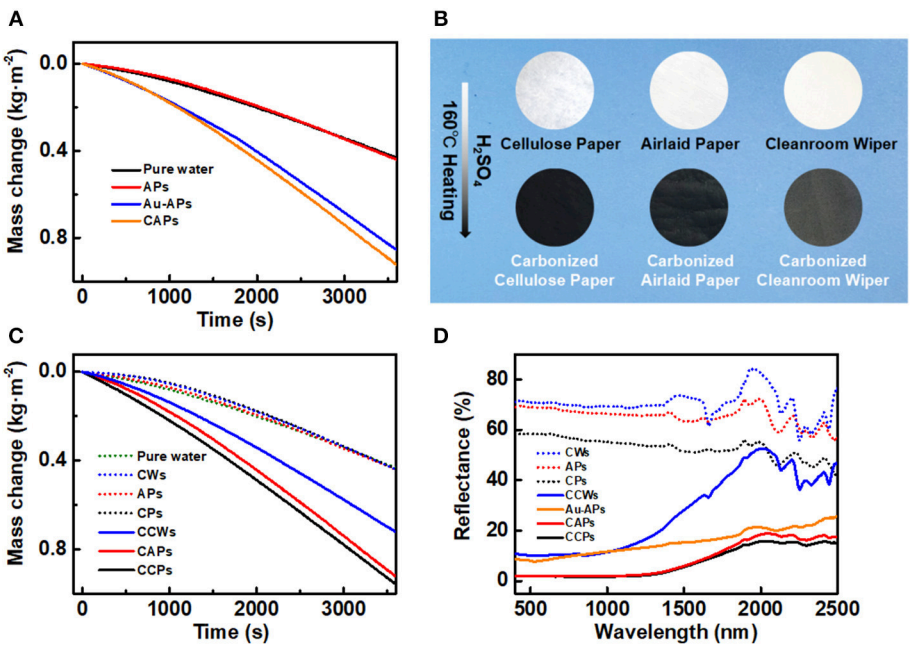

FIGURE 3 | (A) The typical curves of the mass change vs. time for pure water, APs, Au-Aps, and CAPs under 1 sun illumination. **(B)** The photographs of APs, CAPs, CPs, CCPs, CWs, and CCWs. **(C)** The typical curves of the mass change vs. time for pure water, APs, CAPs, CPs, CCPs, CWs, and CCWs under 1 sun illumination. **(D)** The reflectance spectra of Au-APs, APs, CAPs, CPs, CCPs, CWs, and CCWs.

cellulose, cellulose papers) and CWs (100% polyester, cleanroom wipers) would be chosen as the sources to prepare various CMs in the same way, which was labeled as CCPs (carbonized cellulose papers) and CCWs (carbonized cleanroom wipers), respectively (**Figure 3B**).

As shown in **Figure 3C**, the average evaporation rates of the various CMs under the solar illumination of 1 sun were measured to be 0.924 (CAPs), 0.959 (CCPs), and 0.722 (CCWs) $kg{\cdot}m^{-2}{\cdot}h^{-1}$, respectively, which were about 1.7∼2.2 times compared with those of the pure water (0.431 $kg{\cdot}m^{-2}{\cdot}h^{-1}$), APs

(0.440 kg·m^{-2}·h^{-1}), CPs (0.438 kg·m^{-2}·h^{-1}), and CWs (0.440 kg·m^{-2}·h^{-1}) (**Table 1**, **Supplementary Table S1**). In particular, the evaporation rates of the CCPs were higher than all other CMs. Such high evaporation rates of CCPs could be attributed to multiple advantages such as strong absorption (low reflectance) due to the carbonization, rapid transport of vapor/liquid because of the porous structure, and restricted thermal diffusion ascribed to low thermal conductivity (Liu et al., 2015c; Hu et al., 2017; Lin et al., 2018).

The strong light absorption is one of the most important conditions for the light-to-heat conversion which could be measured by the UV-Vis diffuse reflectance spectra (DRS). As illustrated in **Figure 3D** and **Supplementary Table S2**, the reflectance of the APs, CPs and CWs reached up to 65.44, 53.03, and 70.33%, respectively, consistent with the low surface temperature under irradiation. After the carbonization, the reflectance of CAPs, CCPs, and CCWs dramatically decreased to 8.38, 7.34, and 27.57%, respectively. In addition, the transmittance of all the samples were <ca. 2.5% (see **Supplementary Figure S3**), which confirmed the strong absorption (70.86∼92.20%, **Supplementary Table S2**) of the CMs. In particular, the CCPs has obtained the highest absorption of 92.20% compared with other CMs and Au-APs(84.06%), corresponding to the highest evaporation rates of CCPs among all the samples.

TABLE 1 | The water evaporation rates ($\dot{m}$) of various samples and the calculation results of the energy conversion efficiency (η_{ECE}).

Samples	Pure water	Au-APs	APs	CAPs	CPs	CCPs	CWs	CCWs
$\dot{m}$ (kg·m^{-2}·h^{-1})	0.431	0.856	0.440	0.924	0.438	0.959	0.440	0.722
η_{ECE} (%)	29.3	58.7	30.0	63.4	29.8	65.8	29.9	49.4

Moreover, the highly efficient solar steam generation of CMs depended on the temperature of the interface between liquid and vapor, which was considered as one of the most important factors for the water evaporation (Sartori, 2000; Al-Shammiri, 2002). In order to further explore the temperature of the interface affected by the CMs, an IR camera was used to monitor the interfacial temperature vs. time during the solar steam generation (**Figure 4**). After 1 h illumination of 1 sun, the CMs reached the temperature of 40.3°C (CAPs), 41.2°C (CCPs), and 37.5°C (CCWs), respectively, which showed an increase than those of pure water (29.3°C) and the fiber products (29.7∼30.0°C). Especially, the temperature of the CCPs and CAPs was the higher than the Au-APs, supporting their better performance in the water evaporation tests than that of the Au-APs. Meanwhile, the real-temperature changes vs. time for the CCPs under 1 sun showed in **Supplementary Figure S4A**, which certificated a sharper increase than those of pure water and the CPs.

After carbonization, the component of the CMs would be changed, which could be confirmed by the elemental analysis (EA, see **Supplementary Table S3**). Very few contents of the trace metals in the CMs were also tested by the inductively coupled plasma atomic emission spectrometry

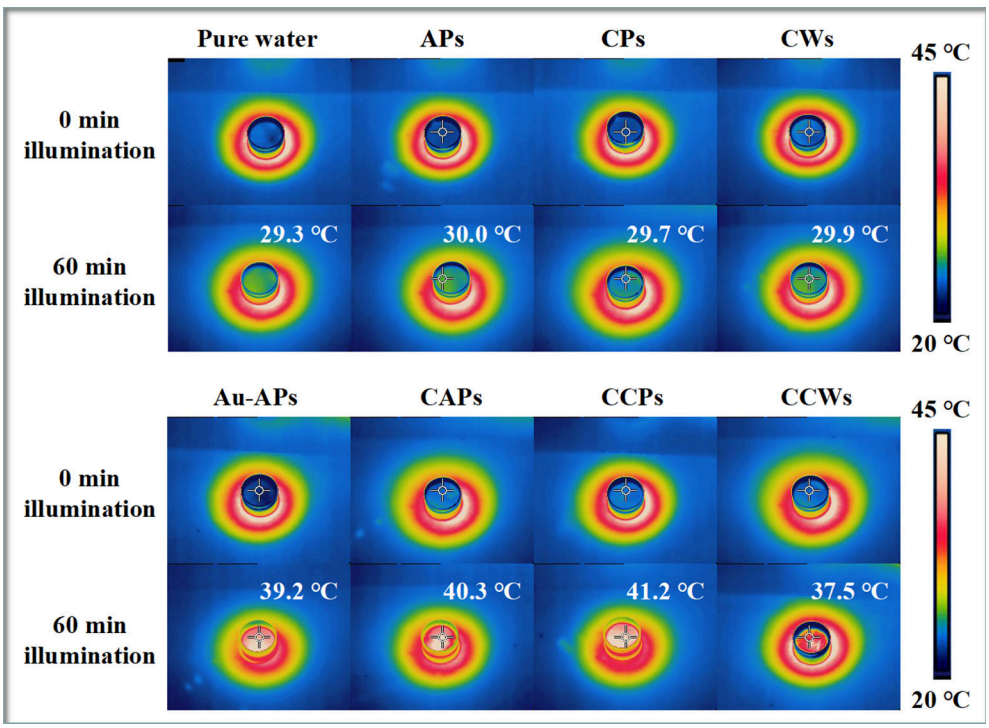

FIGURE 4 | The IR images of temperature changes for the pure water, Au-APs, APs, CAPs, CPs, CCPs, CWs, and CCWs (with water immersion) under 1 sun illumination within 1 h.

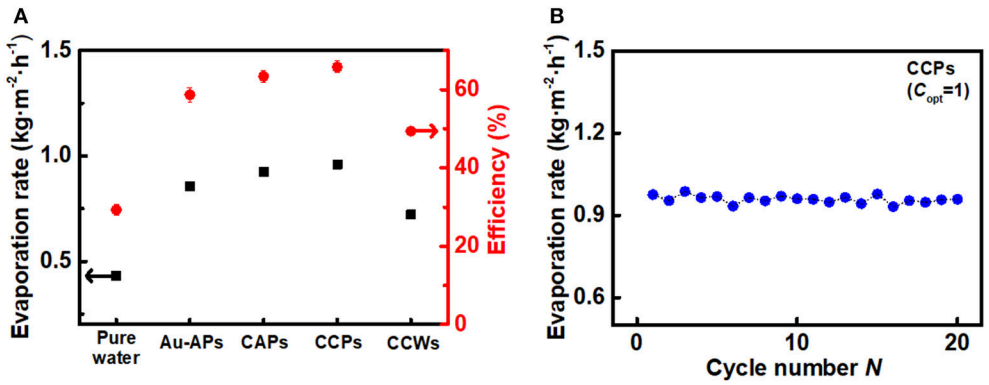

FIGURE 5 | (A) The average evaporation rates (left-hand side axis) with pure water, Au-APs, CAPs, CCPs, and CCWs (black square points) under the solar illumination of 1 sun, together with the corresponding η_{ECE} of pure water, Au-APs, CAPs, CCPs, and CCWs (red circular points, right-hand side axis). **(B)** The recyclability of CCPs under 1 sun illumination by recycling 20 times. Each cycle was tested for 1 h.

(ICP-AES, **Supplementary Table S4**). With the variation of the carbonized degree and the oxidation degree, the decrease of the thermal conductivity of the CMs should probably be attributed to the increase of the C-C (the specra of the C 1s, **Supplementary Figure S6**), the increase of the O-C and the decrease of the -OH (the specra of the O 1s, **Supplementary Figure S7**) after carbonization, which could be verified by and X-ray photoelectron spectroscopy (XPS, see **Supplementary Figures S5–S7**). The thermal conductivities (**Supplementary Table S1**) of the CMs (0.031∼0.058 $W{\cdot}m^{-1}{\cdot}K^{-1}$) were lower than the fiber products (0.119∼0.150 $W{\cdot}m^{-1}{\cdot}K^{-1}$), Au-APs (0.49 $W{\cdot}m^{-1}{\cdot}K^{-1}$) (Liu et al., 2015c), and pure water (0.56 $W{\cdot}m^{-1}{\cdot}K^{-1}$) (Liu et al., 2015c). Compared with other CMs (see **Supplementary Table S1**), the CCPs have the lower thermal conductivity (0.031 $W{\cdot}m^{-1}{\cdot}K^{-1}$), which would be beneficial to restrict the thermal diffusion, leading to the remarkable performance boost of CCPs for solar steam generation.

Based on the aforementioned discussion, the CCPs have shown optimal water evaporation rates among the CMs ascribed to their lower thermal conductivity and better light absorption. In order to evaluate the solar steam generation performance more accurately, the energy conversion efficiency (η_{ECE}) was calculated via the following equation:

$$\eta_{ECE} = \frac{\dot{m}h_{LV}}{C_{opt}P_0} \quad (1)$$

where $\dot{m}$ is the mass flux, h_{LV} is the total enthalpy of the liquid–vapor phase change, P_0 is the normal solar illumination of one sun (1 $kW{\cdot}m^{-2}$), and $C_{\text{opt}}P_0$ refers to the illumination intensity on the absorbers surface (Zhou et al., 2016c). In particular, the calculation of h_{LV} was based on the sensible heat and the temperature-dependent enthalpy of vaporization (see in **Supplementary Table S1**, Liu et al., 2017). The calculated η_{ECE} of solar steam generations under corresponding solar illumination was shown in **Figure 5A** with error bars. The η_{ECE} of CCPs (red circular points) was calculated to be 65.8% under 1 sun illumination, as the best efficiency when compared with other samples (**Table 1**, **Supplementary Table S1**).

Due to the importance of the solar intensity fluctuates as a feature for solar steam generation, as shown in **Supplementary Figure S4B**, the average evaporation rates of the CCPs under the various solar illumination of 1, 2, 3, 4, and 6 sun have been additionally investigated, corresponding to 0.959, 1.877, 2.843, 3.801, and 5.712 $kg{\cdot}m^{-2}{\cdot}h^{-1}$, respectively. They were ca. 2.1 times in contrast with those of the pure water (corresponded to 0.431, 0.883, 1.267, 1.740, and 2.684 $kg{\cdot}m^{-2}{\cdot}h^{-1}$, respectively). In order to obtain better performance of the CCPs, the influence of the CMs' thickness (CCPs with different layers) has been explored (**Supplementary Figure S4C**), which showed that the two-layers CCPs (CCPs-2 layers, 1.057 $kg{\cdot}m^{-2}{\cdot}h^{-1}$) has achieved the best water evaporation rates compared with the single-layers and three-layers CCPs (CCPs-1 layers, 0.954 $kg{\cdot}m^{-2}{\cdot}h^{-1}$and CCPs-3 layers 0.988 $kg{\cdot}m^{-2}{\cdot}h^{-1}$). With the increase of the CCPs' thickness, the water evaporation rates of the CCPs first raised and then decreased a bit, but the results still indicated an enhancement via adding the CCPs' layers. In addition, the recyclability of the solar absorbers was important aspect for efficient solar steam generation. As shown in **Figure 5B**, the recyclability of the CCPs was investigated ($C_{\text{opt}} = 1$, at 25°C and humidity of 50%) that no significant attenuation in evaporation rates was observed for 20 cycles.

CONCLUSIONS

In conclusion, we have demonstrated the use of free-standing porous carbonized-membranes (CMs) derived from the commercial fiber products by one-step carbonization as independent solar absorbers for highly efficient solar steam generation. Our proposed CMs featuring strong absorption, porous structure and low thermal conductivity have shown better evaporation performance compared with the pure water and corresponding original fiber products. As a result, the optimized CMs derived from carbonized cellulose papers (CCPs), achieve the best water evaporation rate of 0.959

$kg{\cdot}m^{-2}{\cdot}h^{-1}$ and the energy conversion efficiency of 65.8% under 1 $kW{\cdot}m^{-2}$ solar illumination, outperforming another CMs and plasmonic airlaid paper (Au-APs). Therefore, the CMs, especially the CCPs, hold great promise as independent solar absorbers for the large-scale application of solar steam generation.

AUTHOR CONTRIBUTIONS

XL wrote the paper. XL and MY carried out the experiments. DY, WH, and XC not only designed the experiments, but also reviewed and revised the paper. All the authors joined discussion about the paper.

ACKNOWLEDGMENTS

This work was supported by the National Natural Science Foundation of China (Grant No. 51573214; 51833011), Guangdong YangFan Innovative & Entepreneurial Research Team Program (Project No. 201633002) and the Youth 1000 Talent Program of China.

SUPPLEMENTARY MATERIAL

The Supplementary Material for this article can be found online at: https://www.frontiersin.org/articles/10.3389/fmats.2018.00074/full#supplementary-material

REFERENCES

Al-Shammiri, M. (2002). Evaporation rate as a function of water salinity. *Desalination* 150, 189–203. doi: 10.1016/S0011-9164(02)00943-8

Bae, K., Kang, G., Cho, S. K., Park, W., Kim, K., and Padilla, W. J. (2015). Flexible thin-film black gold membranes with ultrabroadband plasmonic nanofocusing for efficient solar vapour generation. *Nat. Commun.* 6:10103. doi: 10.1038/ncomms10103

El-Agouz, S. A., El-Aziz, G. A., and Awad, A. M. (2014). Solar desalination system using spray evaporation. *Energy* 76, 276–283. doi: 10.1016/j.energy.2014.08.009

Elimelech, M., and Phillip, W. A. (2011). the future of seawater desalination: energy, technology, and the environment. *Science* 333, 712–717. doi: 10.1126/science.1200488

Ghasemi, H., Ni, G., Marconnet, A. M., Loomis, J., Yerci, S., Miljkovic, N., et al. (2014). Solar steam generation by heat localization. *Nat. Commun.* 5:4449. doi: 10.1038/ncomms5449

Hu, X., Xu, W., Zhou, L., Tan, Y., Wang, Y., Zhu, S., et al. (2017). Tailoring graphene oxide based aerogels for efficient solar steam generation under one sun. *Adv. Mater.* 29:1604031. doi: 10.1002/adma.201604031

Idicula, M., Boudenne, A., Umadevi, L., Ibos, L., Candau, Y., and Thomas, S. (2006). Thermophysical properties of natural fibre reinforced polyester composites. *Compos. Sci. Technol.* 66, 2719–2725. doi: 10.1016/j.compscitech.2006.03.007

Ito, Y., Tanabe, Y., Han, J., Fujita, T., Tanigaki, K., and Chen, M. (2015). Multifunctional porous graphene for high-efficiency steam generation by heat localization. *Adv. Mater.* 27, 4302–4307. doi: 10.1002/adma.201501832

Karagiannis, I. C., and Soldatos, P. G. (2008). Water desalination cost literature: review and assessment. *Desalination* 223, 448–456. doi: 10.1016/j.desal.2007.02.071

Lenert, A., and Wang, E. N. (2012). Optimization of nanofluid volumetric receivers for solar thermal energy conversion. *Sol. Energy* 86, 253–265. doi: 10.1016/j.solener.2011.09.029

Lewis, N. S. (2016). Research opportunities to advance solar energy utilization. *Science* 351:aad1920. doi: 10.1126/science.aad1920

Lin, X., Chen, J., Yuan, Z., Yang, M., Chen, G., Yu, D., et al. (2018). Integrative solar absorbers for highly efficient solar steam generation. *J. Mater. Chem. A* 6, 4642–4648. doi: 10.1039/C7TA08256H

Liu, Y., Chen, J., Guo, D., Cao, M., and Jiang, L. (2015a). Floatable, self-cleaning, and carbon-black-based superhydrophobic gauze for the solar evaporation enhancement at the air-water interface. *ACS Appl. Mater. Interfaces* 7, 13645–13652. doi: 10.1021/acsami.5b03435

Liu, Y., Lou, J., Ni, M., Song, C., Wu, J., Dasgupta, N. P., et al. (2015b). Bioinspired bifunctional membrane for efficient clean water generation. *ACS Appl. Mater. Interfaces* 8, 772–779. doi: 10.1021/acsami.5b09996

Liu, Y., Yu, S., Feng, R., Bernard, A., Liu, Y., Zhang, Y., et al. (2015c). A bioinspired, reusable, paper-based system for high-performance large-scale evaporation. *Adv. Mater.* 27, 2768–2774. doi: 10.1002/adma.201500135

Liu, Z., Song, H., Ji, D., Li, C., Cheney, A., Liu, Y., et al. (2017). Extremely cost effective and efficient solar vapor generation under nonconcentrated illumination using thermally isolated black paper. *Glob. Challenge* 1:1600003. doi: 10.1002/gch2.201600003

Lou, J., Liu, Y., Wang, Z., Zhao, D., Song, C., Wu, J., et al. (2016). Bioinspired multifunctional paper-based rGO composites for solar-driven clean water generation. *ACS Appl. Mater. Interfaces* 8, 14628–14636. doi: 10.1021/acsami.6b04606

Ni, G., Li, G., Boriskina, S. V., Li, H., Yang, W., Zhang, T., et al. (2016). Steam generation under one sun enabled by a floating structure with thermal concentration. *Nat. Energy* 1:16126. doi: 10.1038/nenergy.2016.126

Nyholm, L., Nyström, G., Mihranyan, A., and Strømme, M. (2011). Toward flexible polymer and paper-based energy storage devices. *Adv. Mater.* 23, 3751–3769. doi: 10.1002/adma.201004134

Philibert, C. (2011). *Solar Energy Perspectives*. Paris: International Energy Agency.

Sartori, E. (2000). A critical review on equations employed for the calculation of the evaporation rate from free water surfaces. *Sol. Energy* 68, 77–89. doi: 10.1016/S0038-092X(99)00054-7

Schiermeier, Q. (2008). Water: purification with a pinch of salt. *Nature* 452, 260–261. doi: 10.1038/452260a

Shannon, M. A., Bohn, P. W., Elimelech, M., Georgiadis, J. G., Mariñas, B. J., and Mayes, A. M. (2008). Science and technology for water purification in the coming decades. *Nature* 452, 301–310. doi: 10.1038/nature06599

Wang, G., Fu, Y., Ma, X., Pi, W., Liu, D., and Wang, X. (2017a). Reusable reduced graphene oxide based double-layer system modified by polyethylenimine for solar steam generation. *Carbon* 114, 117–124. doi: 10.1016/j.carbon.2016.11.071

Wang, X., He, Y., Liu, X., Cheng, G., and Zhu, J. (2017b). Solar steam generation through bio-inspired interface heating of broadband-absorbing plasmonic membranes. *Appl. Energy* 195, 414–425. doi: 10.1016/j.apenergy.2017.03.080

Wang, Z., Liu, Y., Tao, P., Shen, Q., Yi, N., Zhang, F., et al. (2014). Bio-inspired evaporation through plasmonic film of nanoparticles at the air–water interface. *Small* 10, 3234–3239. doi: 10.1002/smll.201401071

Xu, Y., Zhu, Y., Han, F., Luo, C., and and Wang, C. (2015). 3D Si/C fiber paper electrodes fabricated using a combined electrospray/electrospinning technique for Li-ion batteries. *Adv. Energy Mater.* 5:1400753. doi: 10.1002/aenm.201400753

Zhou, J., Sun, Z., Chen, M., Wang, J., Qiao, W., Long, D., et al. (2016a). Macroscopic and mechanically robust hollow carbon spheres with superior oil adsorption and light-to-heat evaporation properties. *Adv. Funct. Mater.* 26, 5368–5375. doi: 10.1002/adfm.201600564

Zhou, L., Tan, Y., Ji, D., Zhu, B., Zhang, P., Xu, J., et al. (2016b). Self-assembly of highly efficient, broadband plasmonic absorbers for solar steam generation. *Sci. Adv.* 2:e1501227. doi: 10.1126/sciadv.1501227

Zhou, L., Tan, Y., Wang, J., Xu, W., Yuan, Y., Cai, W., et al. (2016c). 3D self-assembly of aluminium nanoparticles for plasmon-enhanced solar desalination. *Nat. Photonics* 10, 393–398. doi: 10.1038/nphoton.2016.75

Zhou, L., Zhuang, S., He, C., Tan, Y., Wang, Z., and Zhu, J. (2017). Self-assembled spectrum selective plasmonic absorbers with tunable bandwidth for solar energy conversion. *Nano Energy* 32, 195–200. doi: 10.1016/j.nanoen.2016.12.031

Zhu, G., Xu, J., Zhao, W., and Huang, F. (2016). Constructing black titania with unique nanocage structure for solar desalination. *ACS Appl. Mater. Interfaces* 8, 31716–31721. doi: 10.1021/acsami.6b11466

Conflict of Interest Statement: The authors declare that the research was conducted in the absence of any commercial or financial relationships that could be construed as a potential conflict of interest.